Polymer Chemistry

ROYAL SOCIETY OF CHEMISTRY

PAPER

View Article Online
View Journal | View Issue

Cite this: *Polym. Chem.*, 2022, **13**, 3806

Taking advantage of β-hydroxy amine enhanced reactivity and functionality for the synthesis of dual covalent adaptable networks†

Dimitri Berne, Guilhem Coste, Roberto Morales-Cerrada, Marine Boursier, Julien Pinaud, Vincent Ladmiral * and Sylvain Caillol *

This study demonstrates the advantage of using β-hydroxy amine monomers for the synthesis of CANs. The increased reactivity of β-hydroxy amines towards the aza-Michael addition compared to their alkyl equivalents was highlighted by kinetic analyses coupled with rheological experiments. New catalyst-free covalent adaptable networks (CANs) were thus synthesized by poly aza-Michael addition using either β-hydroxy amine or its non-hydroxy analog. These CANs exhibit dynamic aza-Michael exchange under thermal stimulus. The synergistic effect of exchange reactions was highlighted by stress-relaxation and frequency sweep analyses. CANs were finally reshaped and their chemical and physical properties were compared to the initial ones.

Received 1st March 2022,
Accepted 4th June 2022

DOI: 10.1039/d2py00274d

rsc.li/polymers

Introduction

Polymers are designed according to the targeted applications and can be classified into three categories: thermoplastics, thermosets and elastomers. Thermoplastics are composed of entangled linear polymer chains, and are reprocessable by thermal treatment and soluble in suitable solvents. In contrast, thermosets are three-dimensional networks composed of polymer chains cross-linked by covalent bonds, giving these materials strong mechanical properties and chemical resistance. However, thermosets are not easily recycled, which is opposed to the current environmental trend of reducing or eliminating waste production.[1] In this context, covalent adaptable networks (CANs) allowing the production of "recyclable thermosets" are gaining increasing attention. These polymer materials are three-dimensional networks but include exchangeable bonds giving them reprocessing properties under pH, light or thermal stimuli.[2–4]

The concept of CAN was pioneered decades ago[5–7] and revisited recently[8] on a cross-linked rubber that incorporated disulfide linkages as reversible covalent bonds enabling the reprocessing of the polymer network. Numerous exchange reactions have been developed to broaden the scope of CANs, as reported in recent reviews.[9,10] Among them, Diels–Alder addition,[11–14] thiol–ene addition,[15,16] triazolinediones (TAD) chemistry,[17,18] transesterification,[19–21] transamination,[22,23] transcarbamoylation,[24] transimination,[25] and boronate metathesis[26] have been the most studied so far. Other CANs have also been based on disulfide exchange,[27,28] alkoxyamine bond dissociation,[29] transalkylation,[30] transacetalation,[31] transamidation[32] or acid exchange.[33,34]

Most of these exchange reactions usually require catalysts to be activated under thermal stimulus.[35] The presence of these catalysts can potentially cause leaching, ageing and sintering issues.[36,37] To avoid the presence of catalyst in CANs, neighbouring group participation (NGP) and internal catalysis strategies (often *via* electronic effects) have been recently developed.[9,38] For instance, transesterification rate has been accelerated by the presence of a hydroxyl group in β-position of the ester function in epoxy Zn-catalyzed vitrimers.[2,39] Transesterification was also promoted by the incorporation of carboxylic or sulfonic acids close to the ester function (although this modification can lead to a dissociative mechanism).[40,41] Our group also recently highlighted the possibility to use fluorine groups as accelerating electrostatic substituents in transesterification vitrimers.[42] Other strategies consist in the incorporation of amino groups in CANs to promote the transesterification of di(*o*-aminophenylboronic)[43] and silyl-ether exchange[44] for example. Finally, Du Prez *et al.* interestingly demonstrated that the presence of β-amino ester allows catalyst-free transesterification *via* NGP.[45]

Recently, Dichtel and Elling reported that the use of vitrimers alone would not solve the current industrial recycling challenges and that CANs coupling associative and dissociative mechanisms should be developed to achieve these objectives.[46] In this context, some authors have interestingly developed materials using associative and dissociative exchange

ICGM, Univ Montpellier, CNRS, ENSCM, Montpellier, France.
E-mail: vincent.ladmiral@enscm.fr, sylvain.caillol@enscm.fr

†Electronic supplementary information (ESI) available: NMR, FTIR and frequency sweep analyses. See DOI: https://doi.org/10.1039/d2py00274d

reactions to decrease both relaxation and reprocessing times. For instance, Zhang *et al.* developed a CAN combining disulfide metathesis and carboxylate transesterification.[47] Thiol chemistry has also been used to develop materials combining associative and dissociative pathways.[48,49] Lately, the reversible character of the aza-Michael addition was demonstrated by kinetic experiments on model molecules.[45] This new exchange reaction was then synergistically used with transesterification in CANs produced from pentaerythritol triacrylate and commercial diamines.[45] This initial work demonstrated the potential of aza-Michael exchange but was in a way structurally limited by the need of hydroxyl group on acrylate monomers. Moreover, the parameters influencing aza-Michael addition have not been explored in this initial study.

Our group recently studied the reactivity of β-hydroxy amines and demonstrated their higher reactivity compared to regular amines. This effect was observed for the addition of amine on both epoxy[50] and cyclocarbonate.[51] Moreover, β-hydroxy amines can easily be obtained from biobased epoxy monomers. Here, inspired by the work of Du Prez *et al.*,[45] β-hydroxy amines were used to prepare CANs containing β-amino esters as they represent an innovative way to bring hydroxyl group in a transesterification material. First, the reactivity of β-hydroxy amines toward the aza-Michael addition was kinetically evaluated from a molecular and macromolecular point of view, enabling to gain understanding on the activation of this reaction. Then, aza-Michael addition was employed to synthesize new CAN capable of transesterification and exchange *via* aza-Michael additions. Next, insolubility, reshaping and relaxation properties were studied for this dual aza-Michael/transesterification CAN.

Results and discussion

Kinetic study

Kinetic studies were carried out with model molecules in order to determine the influence of β-hydroxy amine on the aza-Michael addition rate. Two model molecules were chosen: *n*-butylamine (Scheme 1a) and 1-amino-2-butanol (Scheme 1b). Butylacrylate was selected as Michael acceptor since it exhibits a high reactivity (notably higher than that of methacrylates) in aza-Michael addition among α,β-unsaturated carbonyl-containing compounds.[52]

First, reactions were performed using acrylate : amine stoichiometric ratios 2 : 1 since both primary and secondary amines can react with acrylate double bonds. In addition, to study the influence of an excess of amine protons compare to the acrylate function, a kinetic study was carried out with excess amine (acrylate : amine 1 : 1). Reagents, equivalents of each reagent and the conversion of the acrylate functions after 15 h of reaction are summarized in Table 1.

The disappearance of the double bond of the acrylate at 35 °C was monitored by ^{1}H NMR spectroscopy (*e.g.* Fig. S1†). Additionally, the ^{1}H NMR peaks assignment of the adducts formed during the aza-Michael reaction of butylacrylate and *n*-butylamine (entry 4) are exhibited in Fig. 1. As shown in Fig. 2, the conversion of the butylacrylate double bond *via* aza-Michael addition with *n*-butylamine (entry 1) progressed slower than with 1-amino-2-butanol (entry 2). After 5 h of reaction, the β-hydroxy amine led to almost 40% conversion of

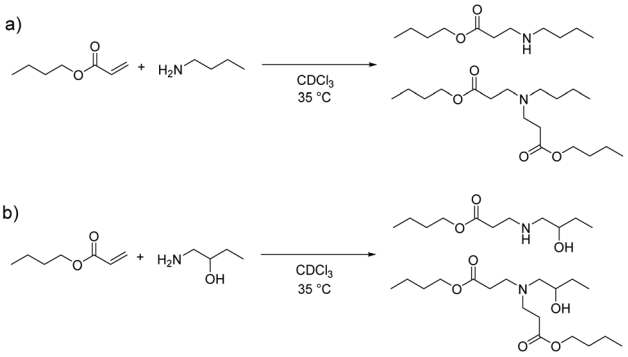

Scheme 1 Reaction of butylacrylate with (a) *n*-butylamine and (b) 1-amino-2-butanol in the presence of 1,3,5-trioxane (internal standard) in $CDCl_3$ at 35 °C.

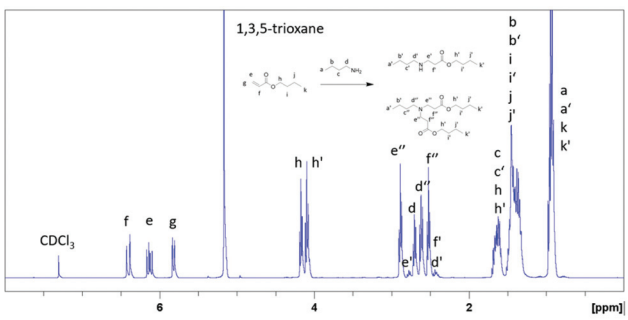

Fig. 1 ^{1}H NMR spectrum of the reaction media corresponding to entry 4 ($CDCl_3$, 400 MHz) at t = 24 h.

Table 1 Equivalents of *n*-butylamine, 1-amino-2-butanol, butylacrylate and ethanol of entries 1 to 5 and conversion of the acrylate bond at t = 15 h

Entry	*n*-Butylamine (eq.)	1-Amino-2-butanol (eq.)	Butylacrylate (eq.)	Ethanol (eq.)	Conversion at t = 15 h (%)
1	1	0	2	0	37
2	0	1	2	0	52
3	1	0	2	1	55
4	1	0	1	0	27
5	0	1	1	0	43

acrylate bonds, whereas the reaction with *n*-butylamine only reached 20% conversion. The reaction of *n*-butylamine and butylacrylate was also carried out in the presence of ethanol (2 : 1 : 1 butylacrylate : *n*-butylamine : ethanol, entry 3). At the beginning of the reaction, the β-hydroxy amine reacted faster than *n*-butylamine in the presence of ethanol. After 7.5 h, the trend was reversed and the *n*-butylamine/ethanol mixture led to slightly higher conversion than 1-amino-2-butanol. Nevertheless the acrylate reacted faster when hydroxyl groups were present in the reaction medium. These results show that hydroxy groups accelerate the Michael addition of amines on acrylates but whether they are located on the beta carbon of the amines or free in solution (as alcohol) may not be significant. Accordingly, two mechanisms can be accounted for the acceleration of the reaction by the OH group: (i) activation of the carbonyl by H-bonding or (ii) participation of the OH in the proton transfer step similarly to the cyclocarbonate/β-hydroxy amine addition.[51] In any case, these results suggest that the use of β-hydroxy amine could allow fast aza-Michael addition in bulk thanks to the catalytic effect of the hydroxyl group.

Fig. 3 displays the evolution of the acrylate double bond conversion with time during the aza-Michael addition of *n*-butylamine or 1-amino-2-butanol carried out at different acrylate/amine molar ratios (entries 1, 2, 4 and 5 in Table 1). One primary amine function can react twice with an acrylate. Regardless of the amine, the aza-Michael additions carried out with one equivalent of acrylate functions per one equivalent of N–H bonds (entries 1 and 2) were faster than their counterpart performed using a 1 : 2 acrylate : N–H bonds ratio from *n*-butylamine (entries 4 and 5). This expected behavior is explained by the higher concentration of aza-Michael acceptor, which has a strong influence on the kinetics. On the other hand, the kinetic study performed with one equivalent of butylacrylate and two equivalents of N–H bonds of 1-amino-2-butanol (entry 5) remains faster than the one performed with one equivalent of N–H functions of *n*-butylamine and one equivalent of butylacrylate (entry 1). Thus, stoichiometric amounts of acrylates and N–H bonds (entries 1 and 2) were chosen to carry out the synthesis of the materials presented in this work.

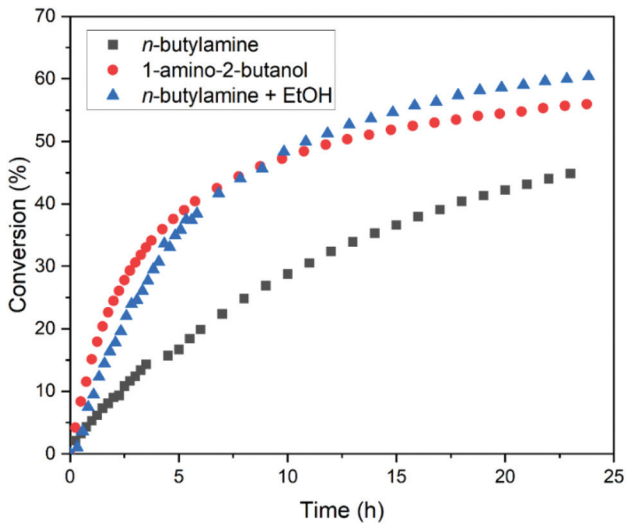

Fig. 2 Conversion of *n*-butylacrylate double bonds *versus* time in the presence of *n*-butylamine (entry 1, black square), 1-amino-2-butanol (entry 2, red dot) or *n*-butylamine with EtOH (entry 3, blue triangle). All these reactions were carried out using one equivalent of acrylate functions and one equivalent of N–H bonds.

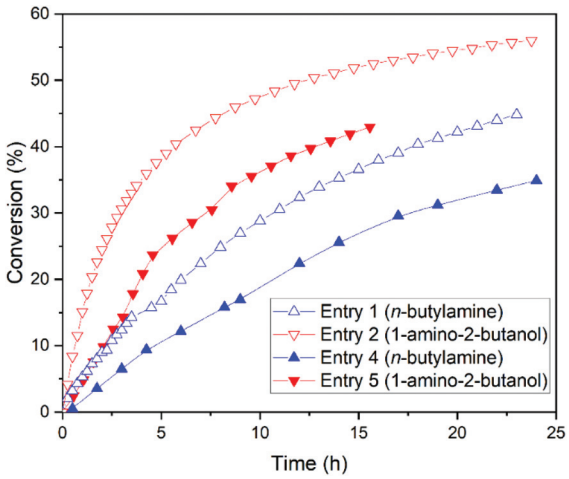

Fig. 3 Conversion *vs.* time for the aza Michael addition of butyl acrylate and *n*-butylamine (blue triangle) or 1-amino-2-butanol (inverted red triangle) carried out using 1 : 1 (full symbols) and 2 : 1 (open symbols) NH motif : acrylate.

Synthesis of the materials

To demonstrate the potential of β-hydroxy amines for the fast synthesis of CANs, pentaerythritol tetraacrylate (PTA) was reacted with two mono functional amines, one possessing a β-hydroxy group, and one deprived of such hydroxy group (Scheme 2). Butylamine and 1-amino-2-butanol were used in this study because they are commercially available and have relatively simple structures. Moreover, since the two hydrogen atoms of the amine function can perform aza-Michael additions, primary monoamines were used as di-functional Michael donors. Therefore, by combining these primary amines with PTA a three-dimensional network can be obtained. The material syntheses were carried out in bulk at 50 °C overnight, with a ratio of two equivalents of acrylate function for one equivalent of amine function. β-Hydroxy amino networks (**BHAN**) and alkylamino networks (**AN**) were respectively prepared from 1-amino-2-butanol and butylamine. PTA possesses ester functions and the use of β-hydroxy amines introduces hydroxy groups in the network structure. Therefore in **BHAN**, transesterification and aza-Michael exchange reactions may occur. In contrast, in **AN** (deprived of hydroxy groups) only aza-Michael exchange may take place.

Model reactions demonstrated that β-hydroxy amines are more reactive than alkylamine in aza-Michael additions. The curing reaction at 50 °C of the two systems was thus monitored by rheometry to confirm this observation on model molecules

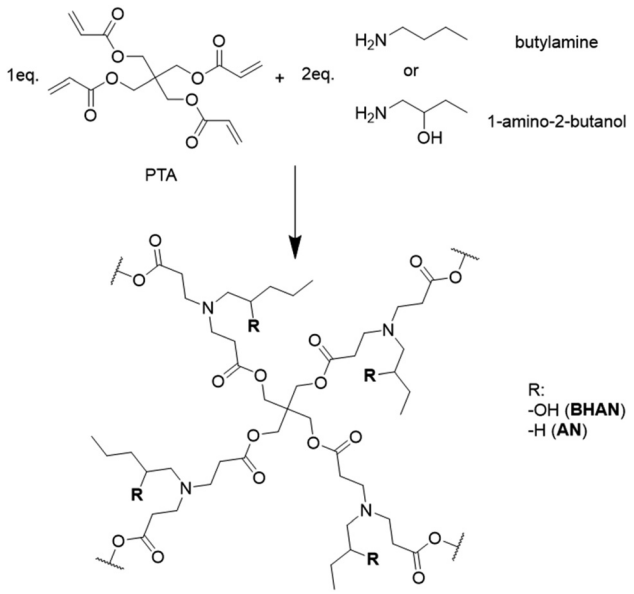

Scheme 2 Synthesis of **AN** and **BHAN** networks.

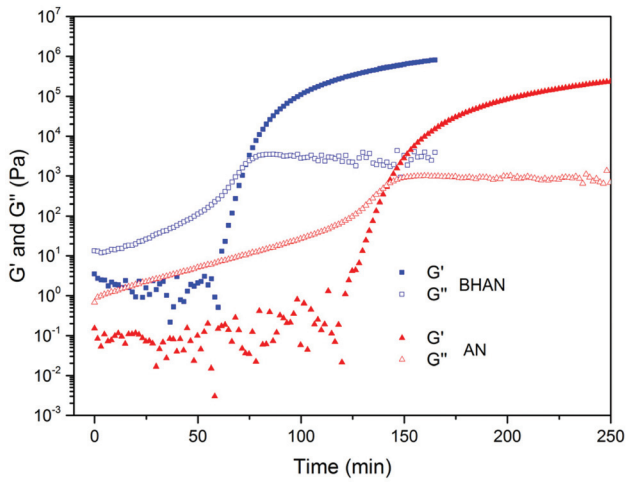

Fig. 4 Evolution of G' and G'' with curing time for **BHAN** (blue squaress) and **AN** (red triangle) formation at a curing temperature of 50 °C.

(Fig. 4). **BHAN** showed a gel point time of 1.2 h, twice lower than that of **AN** (2.4 h). As seen on the model compounds, β-hydroxy amines thus also showed higher reactivity than their non hydroxylated analogs during network formation. The same reasons as those developed in the kinetics part can be used to explain the difference of reactivity between β-hydroxyamine and alkylamine. In **BHAN**, hydroxy groups likely act as internal catalyst for the aza-Michael addition.

The networks were cured at 50 °C overnight and then assessed using both chemical and mechanical analyses. Both materials were translucent. However, **AN** had a slight yellow color compared to **BHAN** (Fig. 10) likely caused by a slight oxydation of the amine. In order to confirm the network synthesis, swelling tests were carried out in THF (Table 2). The

Table 2 Materials characterization

CAN	$T_{d\ 5\%}$ (°C)	Swelling index (%)	Insoluble ratio (%)[a]
BHAN	261	150	94
BHAN-reshaped	245	119	88
AN	264	160	92
AN-reshaped	257	142	84

[a] Insolubility tests were performed in THF at room temperature for 24 h.

swelling index of **AN** was slightly higher than that of **BHAN**. This difference could be explained by a higher network density in **BHAN** caused by H-bonds interactions or by a lower conversion of the acrylate functions in **BHAN**. However, no clear difference was observed between **BHAN** and **AN** by FTIR analysis and no residual enthalpy peak was observed during DSC analysis for both materials, leading to the conclusion that the swelling index difference is likely caused by the formation of H-bonds in BHAN.[53] For both materials, the insoluble ratio were higher than 90% confirming the network formation.

Glass transition temperatures (T_g) were determined by differential scattering calorimetry (DSC), **BHAN** and **AN** showed T_g values of 5 °C and of −17 °C respectively. The higher T_g of **BHAN** is related to the higher number of hydrogen interactions in the material compared to **AN**, which reduces the mobility of the chains. Dynamic mechanical analyses (Fig. 5) revealed T_α values of 24 °C and −2 °C for **BHAN** and **AN** respectively, in agreement with the DSC results. Unsurprisingly, given their structural similarity, **BHAN** and **AN** had similar storage modulus values on the glassy and rubbery plateau (Fig. 5).

TGA analysis showed a 5% weight loss temperature around 260 °C for both materials (Fig. 6 and Table 2). The dissociation of aza-Michael adduct was observed between 260 °C and 380 °C. Indeed, in this temperature range, the adducts obtained after retro-aza Michael could decompose and be

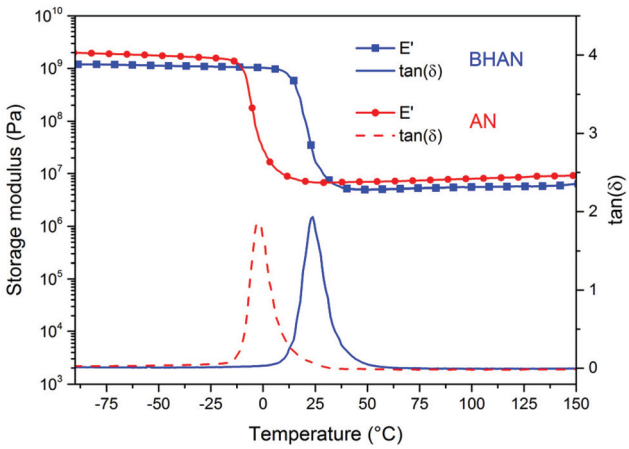

Fig. 5 Storage modulus (E') and tan(δ) of **BHAN** (full blue square and full blue curve) and **AN** (full red circle and red dashed curve).

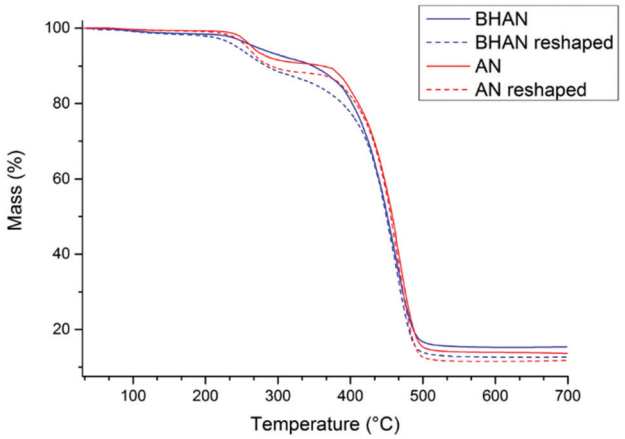

Fig. 6 TGA of AN (red curves) and BHAN (blue curves) before (full lines) and after (dashed lines) reprocessing.

removed from the material.[45] Therefore, the reprocessing temperature was chosen significantly lower than the decomposition temperature to avoid significant loss of properties during reprocessing.

Dynamic properties

The dynamic properties of the materials were evaluated by stress relaxation experiments. A 5% torsional strain was applied and the relaxation modulus ($G(t)$) was monitored as a function of time. Relaxation experiments were performed at temperatures ranging from 130 to 190 °C for both **BHAN** (Fig. 7) and **AN** materials (Fig. 8). Non-normalized relaxations are respectively provided in Fig. S2 and S3† for **BHAN** and **AN**. **BHAN** is expected to relax faster than **AN** since it is contains both ester and hydroxy groups whereas only ester functions are present in **AN**. Hence, both materials may undergo retro-aza Michael/aza Michael exchange but only **BHAN** can also undergo transesterification.

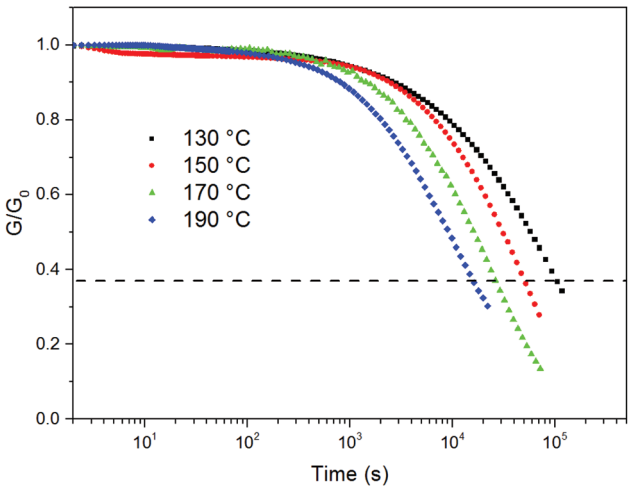

Fig. 8 Normalized stress-relaxation curves at temperatures ranging from 130 to 190 °C for **AN**.

Relaxation times (τ) were shorter for **BHAN** than for **AN** For instance at 130 °C, τ = 17.6 h and τ = 29.2 h were obtained for **BHAN** and **AN** respectively. Two reasons can be hypothesized to explain these results: first, in **AN** only aza-Michael exchange reactions can take place while in **BHAN** transesterification exchanges are also possible due to the presence of hydroxy groups. In addition, the rate of transesterification was shown to be higher than the exchange rate *via* aza-Michael reactions.[45] Secondly, it was also demonstrated[48,49] that the use of a combination of exchange reactions entails a synergistic effect for the relaxation of the material and the reshaping temperature required. Finally, it can also be hypothesized that the presence of the hydroxy group favours the retro-aza Michael as H-bond presence could stabilize the ammonium formed after the dissociation step.

BHAN and **AN** relaxation times followed an Arrhenius behaviour in the studied temperature range (Fig. 9). Flow acti-

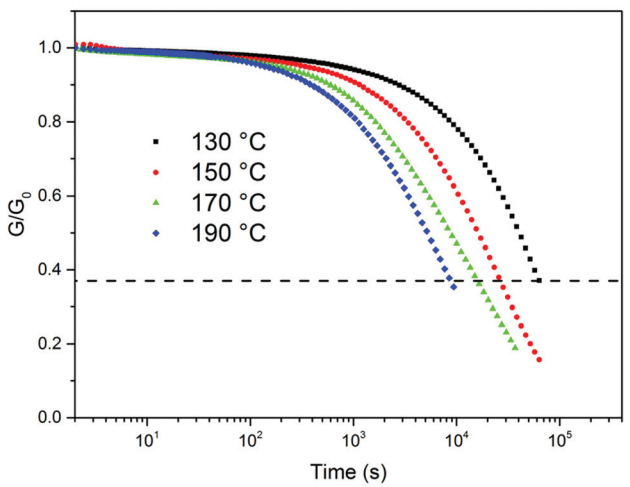

Fig. 7 Normalized stress-relaxation curves at temperatures ranging from 130 to 190 °C for **BHAN**.

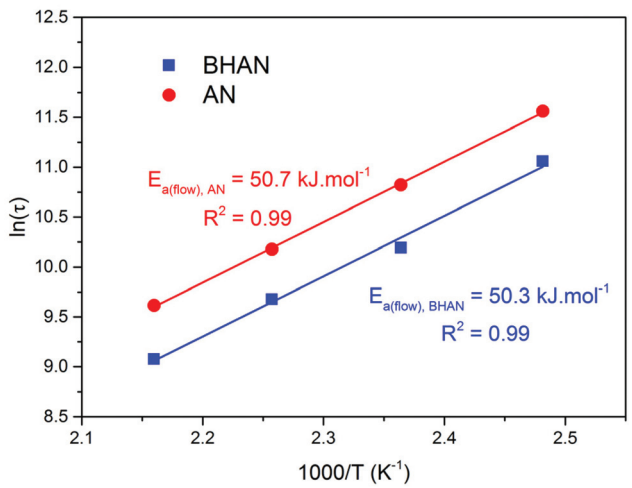

Fig. 9 Fitting of the relaxation times (τ) *vs.* temperature data by the Arrhenius equation for **BHAN** (blue squares) and **AN** (red circle).

vation energies of 50.3 and 50.7 kJ mol^{-1} were determined for **BHAN** and **AN** respectively. These values cannot be easily compared due to the number of concomitant effects in the materials. Indeed, Du Prez *et al.* were also not able to figure out a specific trend for $E_{a(flow)}$ in their initial studies on β-amino esters. Nevertheless, these $E_{a(flow)}$ are relatively low compared to others $E_{a(flow)}$ reported in the literature[9] and could be associated to the use of relatively low molar mass monomers which induces a high density of functionalisation in the network and thus a potentially facilitated exchange.

It should be noted that Arrhenius behaviour was not expected for these materials as aza-Michael exchange proceeds *via* a dissociative mechanism. Nevertheless, Montarnal *et al.* demonstrated that dissociative CANs can show Arrhenius behaviour in a specific temperature range.[54] These results may be ascribed to the fact that the retro aza-Michael proceeds much slower than the aza-Michael addition under these experimental conditions. Therefore, the material can relax the applied stress with only a weak influence on the cross-link density.[55] This hypothesis is confirmed by the fact that the initial relaxation modulus (G_0) is not impacted by the temperature (Fig. S2 and S3†). Frequency sweep data performed at temperature ranging from 120 °C to 180 °C also demonstrate a constant storage modulus, confirming that network connectivity was not dependent of the temperature (Fig. S4 for AN and S5† for BHAN).

Reprocessing properties

These two catalysts-free materials were submitted to reshaping. **BHAN** and **AN** were fragmented and compressed for 2 h under 3 tons at 150 °C and 180 °C respectively (Fig. 10). Higher temperatures were required for **AN** as its relaxation was slower than that of **BHAN** at a given temperature. The thermo-mechanical properties of the materials observed before and after reshaping were compared (Table 2). No clear visual degradation of the materials was observed after reshaping. Both materials remained translucent although **AN** acquired a slight yellow tint. Fig. 6 shows the TGA thermograms of the cured and reshaped **AN** and **BHAN** samples, from 30 °C to 700 °C. Mass loss profiles were not affected by the reshaping procedures, indicating that materials were not significantly impacted by this procedure. Moreover, the FTIR data confirmed that the chemical compositions of the networks were not affected by the reshaping process (Fig. S6 and S7†). Finally, high insoluble fractions (>84%) were obtained on reprocessed samples even if a slight decrease was observed for both materials (Table 2). These relatively lower values may be attributed to the dissociative nature of the aza-Michael exchange reactions.

Dynamic mechanical analyses were also performed to test whether the capacity of the network to relax stress was retained after reshaping. Therefore, frequency sweep measurements were performed from 0.1 to 100 rad s^{-1} at 180 °C for **BHAN** (Fig. 11) and **AN** (Fig. S8†). The storage and loss moduli were only slightly affected by the reprocessing, which is coherent with the chemical analyses of the networks. The loss modulus increase at low frequencies is characteristic of the material starting to flow. The conservation of this effect on reshaped samples demonstrated that the capability of the materials to be reprocessed is not lost and that reprocessing cycle could be repeated. The loss modulus increase occurred at lower frequencies for **AN** compared to **BHAN** at 180 °C which is in good agreement with the relaxation times determined earlier.

Experimental

Materials and methods

Pentaerythritol tetraacrylate (purity 99.9%), butyl acrylate (99%), *n*-butylamine (99%), and 1,3,5-trioxane (99%) were purchased from Sigma-Aldrich (Darmstadt Germany). The 1-amino-2-butanol (99%) was purchased from TCI Europe N.V.

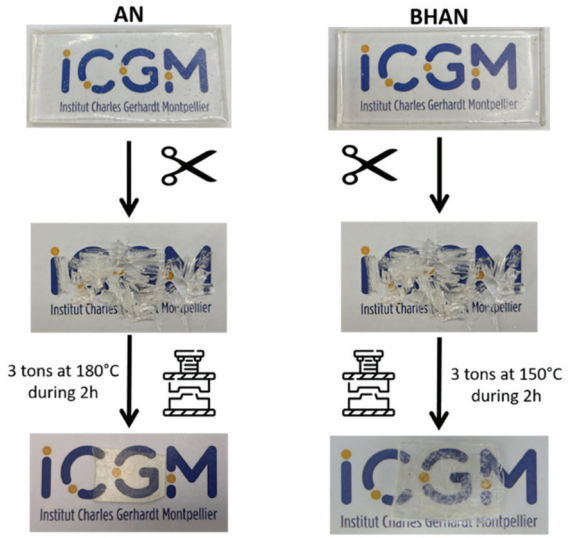

Fig. 10 Reprocessing processes for **AN** (left) and **BHAN** (right).

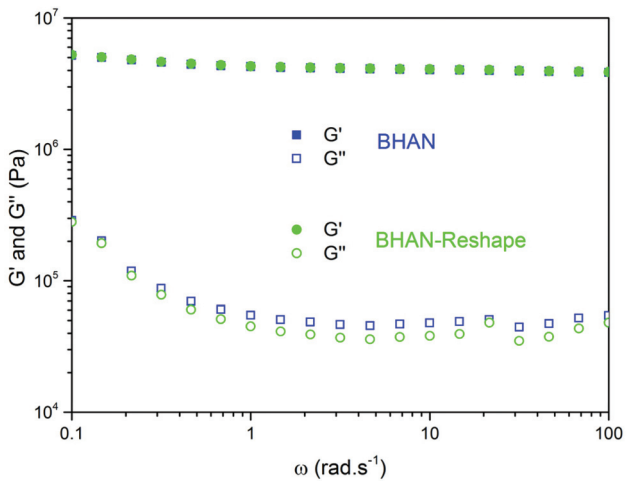

Fig. 11 Measurement of *G′* (full symbol) and *G″* (open symbol) in frequency sweep at 180 °C of **BHAN** (blue squares) and **BHAN** reshape (blue circles).

(Zwijndrecht, Belgium). Ethanol (96%, VWR Chemicals) was purchased from VWR International S.A.S (Fontenay-sous-Bois, France). $CDCl_3$ (99.5%D) was provided by Eurisotop (Saint-Aubin, France). All the materials were used as received.

NMR kinetics

The Nuclear Magnetic Resonance (NMR) spectra were recorded on a Bruker Avance III 400 MHz spectrometer. The instrumental parameters for recording ^{1}H NMR spectra were as follows: flip angle 30°, acquisition time 4.1 s, pulse delay 1.5 s, number of scans 16, and pulse width 5 μs. NMR spectra were recorded without spinning.

As a representative example, for the kinetic study of 2 : 1 acrylate : amine, 73 mg of *n*-butylamine (1 eq.), 21 mg of 1,3,5-trioxane as internal standard and 1 mL of $CDCl_3$ were introduced in a vial (solution 1–1 mol L^{-1} of *n*-butylamine). 256 mg of butylacrylate (2 eq.) and 1 mL of $CDCl_3$ were introduced in another vial (solution 2–2 mol L^{-1} of butylacrylate). For the kinetic studies with 1 : 1 acrylate : amine ratio, 73 mg of *n*-butylamine (1 eq.), 21 mg of 1,3,5-trioxane as internal standard and 1 mL of $CDCl_3$ were introduced in a vial (solution 1–1 mol L^{-1} of *n*-butylamine). 128 mg of butylacrylate (1 eq.) and 1 mL of $CDCl_3$ were introduced in another vial (solution 2–1 mol L^{-1} of butylacrylate). For the kinetic study carried out in the presence of ethanol, 47 mg of ethanol (1 eq.) were added to solution 2. 300 μL of solution 1 were introduced in an NMR tube. A spectrum was recorded at this time (t = 0), and then 300 μL of solution 2 were added to the NMR tube. The NMR tube was vigorously shaken and introduced in the NMR spectrometer thermostated at 35 °C. The conversion of butylacrylate was monitored by ^{1}H NMR (eqn (1)). The signal of 1,3,5-trioxane (internal standard) was integrated from 4.82 ppm to 5.33 ppm. Then the resonance of the double bond of the butylacrylate was integrated from 5.60 ppm to 6.48 ppm. During the first 6 h, a spectrum was recorded every 15 minutes, and then each hour for 24 h.

Conversion determination

$$\text{Conversion}\,(\%) = 1 - \frac{I_t}{I_0} \tag{1}$$

where I_0 and I_t are the values of the integral of the signal of the double bond (5.60 ppm < δ < 6.48 ppm) at t = 0 and t respectively.

The same procedure and the was followed for kinetic reaction.

Fourier transform infrared spectroscopy

Infrared spectra were recorded on a Nicolet 210 Fourier Transform Infrared (FTIR) Spectrometer. The characteristic IR absorptions mentioned in the text are reported in cm^{-1}. Materials analyses were recorded using an ATR accessory.

Thermogravimetric analyses

Thermogravimetric analyses (TGA) were carried out using a Netzsch TG 209F1 apparatus. Approximately 10 mg of sample were placed in an alumina crucible and heated from room temperature to 600 °C at a heating rate of 20 °C min^{-1} under nitrogen atmosphere (40 mL min^{-1}). A nitrogen flow was used to protect the apparatus.

Differential scanning calorimetry

Differential Scanning Calorimetry (DSC) analyses were carried out using a Netzsch DSC200F3 Maia calorimeter, which was calibrated using indium, *n*-octadecane and *n*-octane standards. Nitrogen was used as purge gas. Approximately 10 mg of sample were placed in a perforated aluminum pan and the thermal properties were recorded between −150 °C and 120 °C at 20 °C min^{-1} to observe the glass transition temperature. The T_g values were measured on the second heating ramp to erase the thermal history of the polymer.

Swelling index

Three samples from the same material, of around 40 mg each, were separately immersed in 10 mL of THF for 24 h. The swelling index (SI) was calculated using eqn (2), where m_2 is the mass of the swollen material and m_1 is the initial mass. The reported swelling indices are average values of the 3 independent samples.

Swelling index

$$\text{SI} = \frac{m_2 - m_1}{m_1} \times 100 \tag{2}$$

Gel contents

After the SI measurements, the three samples were dried in a ventilated oven at 80 °C for 24 h. The gel content (GC) was calculated using eqn (3), where m_3 is the mass of the dried material and m_1 is the initial mass. The reported gel contents are the average values of the three samples.

Gel contents

$$\text{GC} = \frac{m_3}{m_1} \times 100 \tag{3}$$

Rheological experiments

Rheology experiments were performed on a Thermo Fisher HAAKE MARS 60 rheometer. The gelation times were measured with a plate-plate geometry with a diameter of 25 mm. The gelation times were analyzed by observing the crossover of the storage modulus (G') and loss modulus (G'') during an oscillatory experiment at 1 Hz, 50 °C and 1% of deformation, according to the previously determined linear domain.

For stress relaxation experiments, a plate-plate geometry with a diameter of 8 mm was used, a strain of 1% was applied to the material and the relaxation modulus ($G(t)$) was monitored over time at a constant temperature. Relaxation curves were fitted with the Kohlrausch–Williams–Watts (KWW) model, which is a stretched exponential function (eqn (4)):

Kohlrausch–Williams–Watts (KWW) model equation.

$$\frac{G(t)}{G_0} = e^{\left(-\frac{t}{\tau}\right)^{\beta}} \tag{4}$$

where τ is the relaxation corresponding to the time needed for the normalized relaxation modulus to decrease to $1/e$ (37%) and β the stretch exponent.

The dependence of the relaxation times with temperature was fitted with the Arrhenius law (eqn (5)):

Arrhenius equation

$$\ln(\tau) = \frac{E_a}{R} \times \frac{1000}{T} - \ln(A) \quad (5)$$

where E_a is the activation energy of the exchange reaction, T the analysis temperature and $R = 8.314$ J mol^{-1} K^{-1}.

DMA

Dynamic mechanical analyses (DMA) were carried out with a Metravib DMA 25 using Dynatest 6.8 software. The samples were tested in uniaxial tension mode while heating at a rate of 3 °C min^{-1} at a frequency of 1 Hz and a fixed strain of 10^{-6} m.

Synthesis of the materials

PTA with butylamine. 1.5 g (1 eq., 20.50 mmol) of butylamine were mixed with PTA (2 eq., 41 mmol) at room temperature. The mixture was then poured into a mold and then cured overnight at 50 °C.

PTA with 1-amino-2-butanol. 1.5 g (1 eq., 16.83 mmol) of 1-amino-2-butanol were mixed with PTA (2 eq., 33.66 mmol) at room temperature. The mixture was then poured into a mold and then cured overnight at 50 °C.

Reprocessing of the vitrimer. Material were initially approximately cut into 2–3 mm squares. Then the reprocessing behaviour of the materials was examined using a Carver 3960 manual heating press. Samples were pressed at a specific temperature for 2 h under 3 tons, and then were cooled to room temperature (*ca.* 20 °C) before removing from the hot press. Rectangular bars were obtained with a height of 20 mm, a width of 10 mm and a thickness of 2 mm.

Conclusions

In the course of this study, higher reactivity rate was observed for β-hydroxy amines compared to their alkyl equivalents during the aza-Michael addition with acrylates. Moreover, complementary analyses highlighted the influence of the hydroxy group on this reaction. These kinetic studies were then confirmed by rheological measurements. Catalyst-free CANs, **BHAN** and **AN**, were thus synthesized by reacting β-hydroxy amine or alkylamine respectively with TPA, a tetraacrylate, at 50 °C.

Both cross-linked materials exhibited aza-Michael exchanges under thermal stimulus. In addition, transesterification exchanges were also possible in the β-hydroxy amine-based networks due to the presence of both ester and hydroxy groups in the material. Stress-relaxation analyses revealed lower relaxation times for the β-hydroxy amine networks due to the combined effects of transesterification and aza-Michael exchanges. Arrhenius behavior was observed for both materials in the temperature range studied. Following the observed trend in dynamic analyses, higher temperature was required to reshape **AN** (180 °C) compare to **BHAN** (150 °C) while the reshaping time and pressure applied remained identical. Finally, chemical and mechanical analyses of the materials before and after reshaping were almost identical, confirming that reprocessing was efficient and did not adversely affect the materials.

To conclude, this study highlights the potential of β-hydroxy amine as building blocks for CANs and paves the way for further applications of these compounds.

Conflicts of interest

There are no conflicts to declare.

Acknowledgements

This work was funded by the French National Research Agency ANR (AFCAN project: ANR-19-CE06-0014).

References

1 J. P. Pascault and R. J. J. Williams, *Handbook of Polymer Synthesis, Characterization, and Processing*, John Wiley and Sons, 2013, pp. 519–533.
2 D. Montarnal, M. Capelot, F. Tournilhac and L. Leibler, *Science*, 2011, **334**, 965–968.
3 P. Chakma, L. H. Rodrigues Possarle, Z. A. Digby, B. Zhang, J. L. Sparks and D. Konkolewicz, *Polym. Chem.*, 2017, **8**, 6534–6543.
4 C. J. Kloxin, T. F. Scott, B. J. Adzima and C. N. Bowman, *Macromolecules*, 2010, **43**, 2643–2653.
5 A. V. Tobolsky, I. B. Prettyman and J. H. Dillon, *Rubber Chem. Technol.*, 1944, **17**, 551–575.
6 M. D. Stern and A. V. Tobolsky, *Rubber Chem. Technol.*, 1946, **19**, 1178–1192.
7 R. C. Osthoff, A. M. Bueche and W. T. Grubb, *J. Am. Chem. Soc.*, 1954, **76**, 4659–4663.
8 P. Zheng and T. J. McCarthy, *J. Am. Chem. Soc.*, 2012, **134**, 2024–2027.
9 F. Cuminet, S. Caillol, É. Dantras, É. Leclerc and V. Ladmiral, *Macromolecules*, 2021, **54**, 3927–3961.
10 M. Guerre, C. Taplan, J. M. Winne and F. E. Du Prez, *Chem. Sci.*, 2020, **11**, 4855–4870.
11 X. Chen, M. A. Dam, K. Ono, A. Mal, H. Shen, S. R. Nutt, K. Sheran and F. Wudl, *Science*, 2002, **295**, 1698–1702.
12 P. Reutenauer, E. Buhler, P. J. Boul, S. J. Candau and J.-M. Lehn, *Chem. – Eur. J.*, 2009, **15**, 1893–1900.
13 B. Zhang, Z. A. Digby, J. A. Flum, E. M. Foster, J. L. Sparks and D. Konkolewicz, *Polym. Chem.*, 2015, **6**, 7368–7372.
14 G. B. Lyon, A. Baranek and C. N. Bowman, *Adv. Funct. Mater.*, 2016, **26**, 1477–1485.

15 N. Kuhl, R. Geitner, R. K. Bose, S. Bode, B. Dietzek, M. Schmitt, J. Popp, S. J. Garcia, S. van der Zwaag, U. S. Schubert and M. D. Hager, *Macromol. Chem. Phys.*, 2016, **217**, 2541–2550.
16 B. Zhang, Z. A. Digby, J. A. Flum, P. Chakma, J. M. Saul, J. L. Sparks and D. Konkolewicz, *Macromolecules*, 2016, **49**, 6871–6878.
17 S. Billiet, K. De Bruycker, F. Driessen, H. Goossens, V. Van Speybroeck, J. M. Winne and F. E. Du Prez, *Nat. Chem.*, 2014, **6**, 815–821.
18 H. A. Houck, K. De Bruycker, S. Billiet, B. Dhanis, H. Goossens, S. Catak, V. Van Speybroeck, J. M. Winne and F. E. Du Prez, *Chem. Sci.*, 2017, **8**, 3098–3108.
19 F. I. Altuna, U. Casado, I. E. Dell'Erba, L. Luna, C. E. Hoppe and R. J. J. Williams, *Polym. Chem.*, 2020, **11**, 1337–1347.
20 F. I. Altuna, C. E. Hoppe and R. J. J. Williams, *RSC Adv.*, 2016, **6**, 88647–88655.
21 M. Hayashi, R. Yano and A. Takasu, *Polym. Chem.*, 2019, **10**, 2047.
22 W. Denissen, G. Rivero, R. Nicolaÿ, L. Leibler, J. M. Winne and F. E. Du Prez, *Adv. Funct. Mater.*, 2015, **25**, 2451–2457.
23 Y. Spiesschaert, C. Taplan, L. Stricker, M. Guerre, J. M. Winne and F. E. Du Prez, *Polym. Chem.*, 2020, **11**, 5377–5385.
24 D. J. Fortman, J. P. Brutman, C. J. Cramer, M. A. Hillmyer and W. R. Dichtel, *J. Am. Chem. Soc.*, 2015, **137**, 14019–14022.
25 A. Chao, I. Negulescu and D. Zhang, *Macromolecules*, 2016, **49**, 6277–6284.
26 M. Röttger, T. Domenech, R. Van Der Weegen, A. Breuillac, R. Nicolaÿ and L. Leibler, *Science*, 2017, **356**, 62–65.
27 M. Liu, J. Zhong, Z. Li, J. Rong, K. Yang, J. Zhou, L. Shen, F. Gao, X. Huang and H. He, *Eur. Polym. J.*, 2020, **124**, 109475.
28 D. J. Fortman, R. L. Snyder, D. T. Sheppard and W. R. Dichtel, *ACS Macro Lett.*, 2018, **7**, 1226–1231.
29 K. Jin, L. Li and J. M. Torkelson, *Adv. Mater.*, 2016, **28**, 6746–6750.
30 M. M. Obadia, B. P. Mudraboyina, A. Serghei, D. Montarnal and E. Drockenmuller, *J. Am. Chem. Soc.*, 2015, **137**, 6078–6083.
31 Q. Li, S. Ma, S. Wang, W. Yuan, X. Xu, B. Wang, K. Huang and J. Zhu, *J. Mater. Chem. A*, 2019, **7**, 18039–18049.
32 F. Van Lijsebetten, Y. Spiesschaert, J. M. Winne and F. E. Du Prez, *J. Am. Chem. Soc.*, 2021, **143**, 15834–15844.
33 D. Boucher, J. Madsen, L. Yu, Q. Huang, N. Caussé, N. Pébère, V. Ladmiral and C. Negrell, *Macromolecules*, 2021, **54**, 6772–6779.
34 D. Boucher, J. Madsen, N. Caussé, N. Pébère, V. Ladmiral and C. Negrell, *Reactions*, 2020, **1**, 89–101.
35 M. Capelot, M. M. Unterlass, F. Tournilhac and L. Leibler, *ACS Macro Lett.*, 2012, **1**, 789–792.
36 J. Wang, S. Chen, T. Lin, J. Ke, T. Chen, X. Wu and C. Lin, *RSC Adv.*, 2020, **10**, 39271–39276.
37 T. Liu, B. Zhao and J. Zhang, *Polymer*, 2020, **194**, 122392.
38 F. Van Lijsebetten, J. O. Holloway, J. M. Winne and F. E. Du Prez, *Chem. Soc. Rev.*, 2020, **49**, 8425–8438.
39 M. Capelot, D. Montarnal, F. Tournilhac and L. Leibler, *J. Am. Chem. Soc.*, 2012, **134**, 7664–7667.
40 M. Delahaye, J. M. Winne and F. E. Du Prez, *J. Am. Chem. Soc.*, 2019, **141**, 15277–15287.
41 H. Zhang, S. Majumdar, R. A. T. M. Van Benthem, R. P. Sijbesma and J. P. A. Heuts, *ACS Macro Lett.*, 2020, **12**, 272–277.
42 D. Berne, F. Cuminet, S. Lemouzy, C. Joly-Duhamel, R. Poli, S. Caillol, E. Leclerc and V. Ladmiral, *Macromolecules*, 2022, **55**, 1669–1679.
43 O. R. Cromwell, J. Chung and Z. Guan, *J. Am. Chem. Soc.*, 2015, **137**, 6492–6495.
44 Y. Nishimura, J. Chung, H. Muradyan and Z. Guan, *J. Am. Chem. Soc.*, 2017, **139**, 14881–14884.
45 C. Taplan, M. Guerre and F. E. Du Prez, *J. Am. Chem. Soc.*, 2021, **143**, 9140–9150.
46 B. R. Elling and W. R. Dichtel, *ACS Cent. Sci.*, 2020, **6**, 1488–1496.
47 M. Chen, L. Zhou, Y. Wu, X. Zhao and Y. Zhang, *ACS Macro Lett.*, 2019, **8**, 255–260.
48 M. Podgórski, N. Spurgin, S. Mavila and C. N. Bowman, *Polym. Chem.*, 2020, **11**, 5365–5376.
49 N. Van Herck, D. Maes, K. Unal, M. Guerre, J. M. Winne and F. E. Du Prez, *Angew. Chem., Int. Ed.*, 2020, **59**, 3609–3617.
50 A.-S. Mora, R. Tayouo, B. Boutevin, G. David and S. Caillol, *Green Chem.*, 2018, **20**, 4075–4084.
51 B. Quienne, R. Poli, J. Pinaud and S. Caillol, *Green Chem.*, 2021, **23**, 1678–1690.
52 A. Genest, S. Binauld, E. Pouget, F. Ganachaud, E. Fleury and D. Portinha, *Polym. Chem.*, 2017, **8**, 624–630.
53 A. S. Mora, R. Tayouo, B. Boutevin, G. David and S. Caillol, *Eur. Polym. J.*, 2020, **123**, 109460.
54 A. Jourdain, R. Asbai, O. Anaya, M. M. Chehimi, E. Drockenmuller and D. Montarnal, *Macromolecules*, 2020, **53**, 1884–1900.
55 O. Anaya, A. Jourdain, I. Antoniuk, H. Ben Romdhane, D. Montarnal and E. Drockenmuller, *Macromolecules*, 2021, **54**, 3281–3292.

